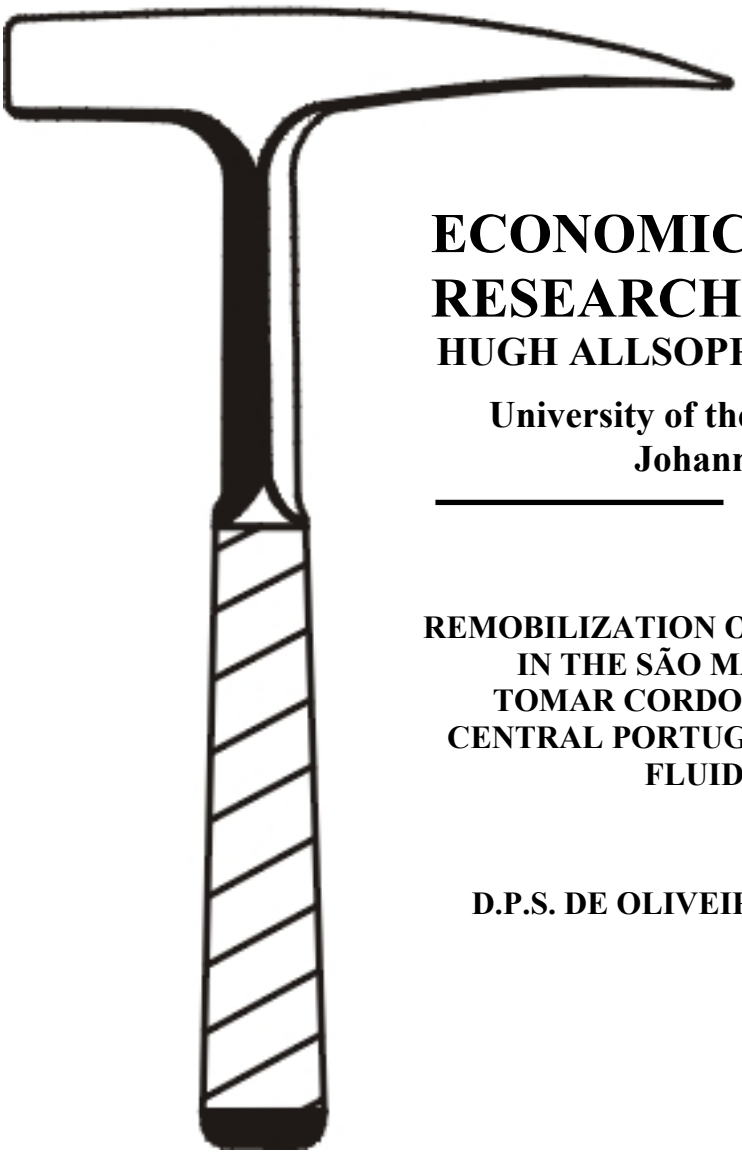

ECONOMIC GEOLOGY RESEARCH INSTITUTE

HUGH ALLSOPP LABORATORY

University of the Witwatersrand
Johannesburg

REMOBILIZATION OF GOLD MINERALIZATION IN THE SÃO MARTINHO PROSPECT, TOMAR CORDOBA SHEAR ZONE, EAST CENTRAL PORTUGAL: CONSTRAINTS FROM FLUID INCLUSIONS

D.P.S. DE OLIVEIRA, Y. YAO and L.J. ROBB

INFORMATION CIRCULAR No. 364

UNIVERSITY OF THE WITWATERSRAND
JOHANNESBURG

REMOBILIZATION OF GOLD MINERALIZATION IN THE SÃO MARTINHO PROSPECT, TOMAR CORDOBA SHEAR ZONE (TCSZ), EAST CENTRAL PORTUGAL: CONSTRAINTS FROM FLUID INCLUSIONS

by

D. P. S. DE OLIVEIRA[1], Y. YAO[2] AND L. J. ROBB[2]

([1] Instituto Geológico e Mineiro, Apartado 7586, 2721-866, Alfragide, Portugal
[2] Economic Geology Research Institute-Hugh Allsopp Laboratory,
School of Geosciences, University of the Witwatersrand,
Private Bag 3, P.O. WITS 2050,
Johannesburg, South Africa)

ECONOMIC GEOLOGY RESEARCH INSTITUTE
INFORMATION CIRCULAR No. 364

December, 2002

REMOBILIZATION OF GOLD MINERALIZATION IN THE SÃO MARTINHO PROSPECT, TOMAR CORDOBA SHEAR ZONE (TCSZ), EAST CENTRAL PORTUGAL: CONSTRAINTS FROM FLUID INCLUSIONS

ABSTRACT

The São Martinho gold prospect provides new insight into the controversial metallogenic proposals (e.g., magmatic vs. metamorphic) for lode gold deposits from various geological settings. The prospect is located within the Tomar Cordoba Shear Zone (TCSZ), an extensive sinistral shear zone extending from Tomar in central Portugal to Cordoba in southwest Spain and which forms the boundary between two tectonostratigraphic zones: the Central Iberian Zone in the north and the Ossa Morena Zone in the south. Two types of gold mineralisation include: (1) a syn-tectonic, disseminated orogenic type (S1), consisting of quartz I (QI), pyrite I and II veinlets, stretched (deformed) pods of arsenopyrite I, chalcopyrite I and gold I with marked chlorite alteration; and (2): a post-tectonic, massive, higher-temperature type (S2), consisting of quartz II (QII), pyrite III, arsenopyrite II (undeformed), pyrrhotite II, loellingite and gold II.

Fluid inclusions in vein quartz from S1 comprise H_2O-NaCl-CO_2-CH_4 (type C) and H_2O-NaCl (type D) inclusions while those from S2 are dominated by hypersaline inclusions bearing daughter minerals (type E). These three types of fluid inclusions are secondary or pseudosecondary in origin. Type C inclusions show average melting and homogenisation temperatures of CO_2 at -64.1 ºC and +2.3 ºC, respectively, and average total homogenisation temperatures to liquid phase at 371 ºC. Type D inclusions average eutectic melting temperatures of -41.7 ºC, ice melting temperatures of -3.6 ºC and a total homogenisation temperature of 129 ºC. Salinities of types C-D inclusions vary between 0.5 and 17.2 wt.% NaCl equivalent, indicating that two types of fluids may have interacted in an open system. Type E fluid inclusions demonstrate melting temperatures of daughter crystals (Tm_{dau}) at 290 to > 550 ºC (median = 400 ºC, n =131), and total homogenisation temperatures to liquid phase at 120 to 470 ºC (median = 290 ºC), which are lower than the Tm_{dau}. Salinities of type E inclusions fall in the range from 32 to >62 wt.% NaCl equivalent.

The fluid inclusion data, together with the geologic setting and ore geology, suggest that the later fluids (represented by type E fluid inclusions) are probably magmatic in origin. The fluids are considered to have been derived from the emplacement of nearby late- to post-Hercynian granitoid bodies (e.g., the Nisa Batholith) and have remobilised originally metamorphic lode gold mineralisation (S1) in the São Martinho prospect. This process resulted in enrichment of gold mineralisation (S2). The hypersaline fluid inclusions are, therefore, a useful tool for regional gold exploration in the Tomar Cordoba Shear Zone.

_____oOo_____

REMOBILIZATION OF GOLD MINERALIZATION IN THE SÃO MARTINHO PROSPECT, TOMAR CORDOBA SHEAR ZONE (TCSZ), EAST CENTRAL PORTUGAL: CONSTRAINTS FROM FLUID INCLUSIONS

CONTENTS

_____oOo_____

Published by the Economic Geology Research Institute
(incorporating the Hugh Allsopp Laboratory)
School of Geosciences
University of the Witwatersrand
1 Jan Smuts Avenue
Johannesburg
South Africa

http://www.wits.ac.za/egru/research.htm

ISBN 1-86838-319-9

REMOBILIZATION OF GOLD MINERALIZATION IN THE SÃO MARTINHO PROSPECT, TOMAR CORDOBA SHEAR ZONE (TCSZ), EAST CENTRAL PORTUGAL: CONSTRAINTS FROM FLUID INCLUSIONS

INTRODUCTION

Orogenic lode gold deposits in Archaean greenstone belts (i.e., shear zones) are one of the major sources of the world's gold production. Although there is general consensus that the gold is transported by hydrothermal fluids and is deposited in chemical and structural traps, there is little consensus on the timing of gold mineralization (Couture et al., 1994; Bierlein and Crowe, 2000). Little is known about the importance of subsequent gold remobilisation processes.

It has been well documented that fluids of lode gold deposits in Archaean to Phanerozoic age are generally CO_2-bearing metamorphic fluids, containing salinities typically <6 wt.% NaCl equivalent (e.g., Bierlein and Crowe, 2000; Hageman and Cassidy, 2000; Yao et al., 2001). Salinities >10 wt.% NaCl equivalent have also been recorded in some of the deposits (e.g., So and Yun, 1997). Occasionally, however, hypersaline fluids, bearing daughter minerals in fluid inclusions, have been reported from lode gold deposits.

Because fluid inclusions in gold quartz veins are characterised by abundant daughter minerals the São Martinho gold prospect provides a good example of where saturated fluids related to gold mineralisation occur. This study demonstrates two definite stages (viz., syn-Hercynian and late- to post-Hercynian) of gold deposition in the São Martinho area, and characterises the hydrothermal fluids related to the two stages of mineralization. The role of the late-stage fluids in remobilization of gold mineralization is discussed.

REGIONAL GEOLOGIC SETTING

The TCSZ is a major NW-SE trending structure (350 x 20 km, Burg et al., 1981) from Tomar in central Portugal to Cordoba in SW Spain and forms the boundary between two major tectonostratigraphic subdivisions of the Iberian Massif (Julivert et al., 1972; Ribeiro et al., 1979): the Central Iberian Zone in the north and the Ossa Morena Zone in the south (Fig. 1, inset). The TCSZ shows intense deformation and metamorphism contemporaneous with a large, intracontinental sinistral fault-produced displacement of 100 km (Burg et al., 1981) to 300 km (Abalos and Eguíluz, 1992) during the Variscan/Hercynian Orogeny (Berthé et al., 1979). The displacement caused mylonitisation and retrograde metamorphism (amphibolite to greenschist facies) to all previous structures and mineral assemblages (Quesada and Munhá, 1990). The TCSZ is also a major Eohercynian-Hercynian sinistral transcurrent fault overprinting a Cadomian arc at a convergent margin of Gondwana (Pereira and Silva, 2001).

The Portuguese sector of the TCSZ comprises a series of polymetamorphic tectonic subdomains (Pereira, 1995), which unconformably overlie a Lower Cambrian carbonate platform sequence in a asymmetric flower structure rooted in the Blastomylonitic Belt forming the core of the shear zone (Pereira and Silva, 1997). More recent studies recognise the existence of several flower-like structures distributed throughout the TCSZ (Pereira, 1999).

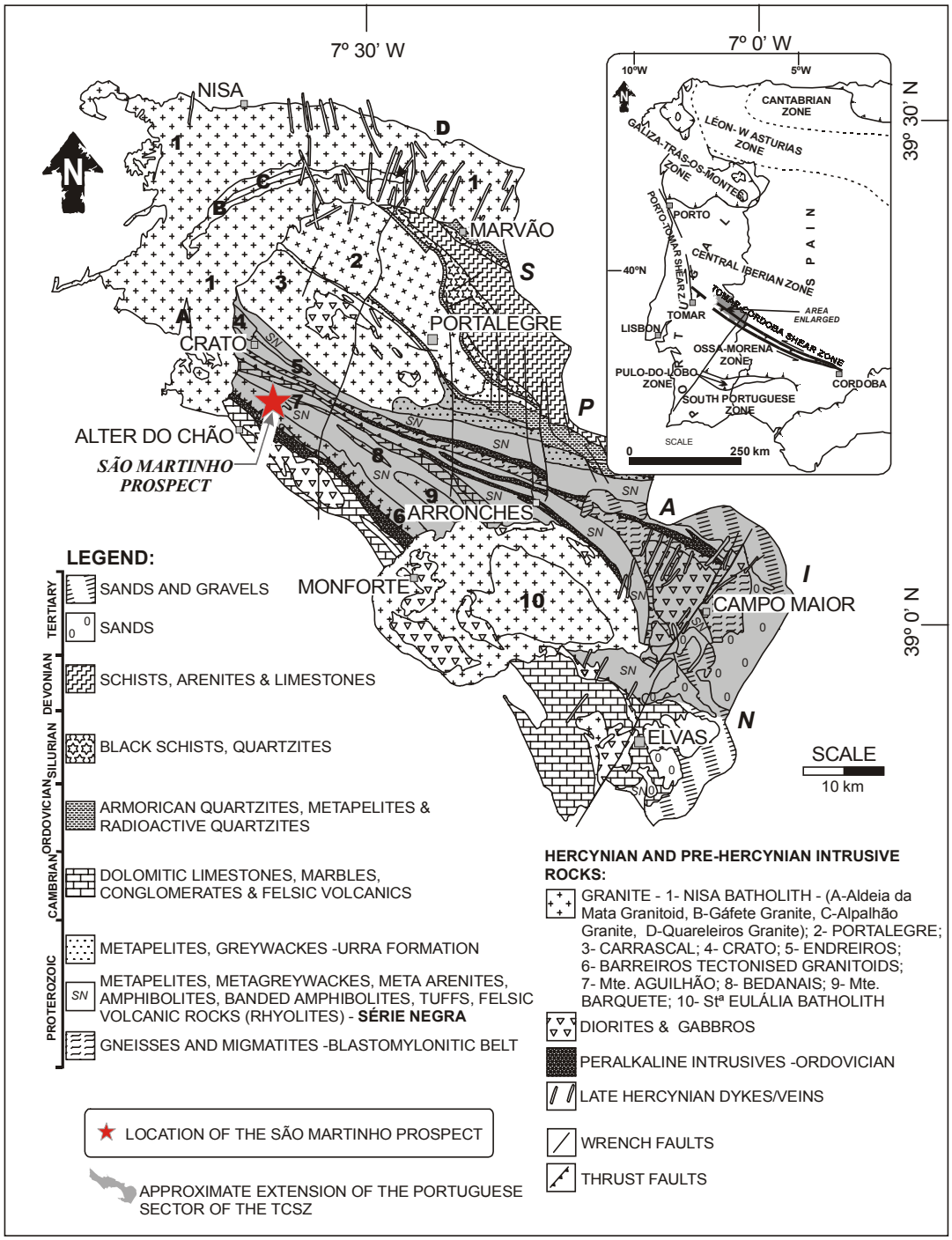

Figure 1: *Excerpt from the 1: 500 000 geological map of Portugal (after Oliveira et al., 1992) showing the location of the São Martinho prospect and surrounding simplified geology. The various granite names with their facies types are reproduced within each granitoid type (where applicable). Nisa granite facies types are after Moreira (1999). Inset shows the extension and location of the TCSZ in relation to the Iberian Massif.*

Figure 2: *Thin rhyolite dykes, intruded into Série Negra (biotite-mica schists), are seen at the intersection of the Navalha stream and Alter do Chão-Porttalegre Station road. These rhyolite units are distal to their source at this locality and are subparallel to Upper Westphalian north-south tension gashes. Further east the dykes are more substantial and in places are greater than 80 m in width.*

The Blastomylonitic Belt (0.45 to 3 km wide), separating greenschist facies rocks to the north from amphibolite facies rocks to the south (Fig. 1), comprises mainly Palaeoproterozoic, migmatitic gneisses (de Oliveira et al., 2002) intruded locally by peridotite, granite and granitic pegmatite veins. The Neoproterozoic, poorly outcropping, gold-enriched Série Negra rocks occur on either side of the Belt. The Belt itself consists of meta-arenites (quartzites), metapelites (schists, metagreywackes), amphibolites, amphibole schists, tuffaceous metasediments, limestones, and rhyolites, which are grouped into the Morenos and Mosteiros Formations. The uppermost Proterozoic Urra Formation occurs stratigraphically above the Série Negra and north of the Blastomylonitic Belt, which is thrust over onto Ordovician quartzites and pelites, thereby juxtaposing Precambrian and Ordovician lithologies in the Central Iberian Zone. The Série Negra is intruded by several felsic bodies (Fig. 1), including pre-Hercynian (Late Cambrian Barreiros granitoids), syn-Hercynian (syntectonic, e.g., Carrascal, Endreiros, Mte. Aguilhão, Bedanais and Mte. Barquete granites, peralkaline intrusives) and late- to post-Hercynian (e.g., the Early Permian-late Carboniferous Nisa granite, and the Permian Stª Eulália granite) granitoids. The peak metamorphism occurred at 340 ± 13 Ma (Ordoñes-Casado, 1998), although the age of metamorphism in the TCSZ is controversial.

The TCSZ and the lithologies bordering the southernmost portion of the Central Iberian Zone show offsets due to Upper Westphalian age (314 - 305 Ma), N-S orientated tension gashes and fractures (Gonçalves et al., 1978). In the São Martinho area, late- to post-Hercynian rhyolite lavas intrude the Série Negra (de Oliveira, 2001a), almost perpendicular to the regional NW-SE-striking foliation. Several smaller rhyolite dykes are parallel to the N-S tension gashes and fractures (Fig. 2). QII veins occur within the rhyolites (see later).

GEOLOGY AND MINERALIZATION AT SÃO MARTINHO

The São Martinho prospect is located south of the Blastomylonitic Belt in amphibolite facies rocks (Fig. 1). Outcrops are scarce due to a large part of the area being covered by a 19 km^2, (on average 1.5m-thick), Palaeogenic, elluvium deposit. This deposit is composed of common angular- to sub-angular pale quartzite and rare amphibolite clasts and appears to be sub-economic, with an average grade of 256 mg Au per. sq. metre, and an average depth of overburden of 0.93m (Camm, 1996). Pale quartzites, granitoid pods and lenses and amphibolites suboutcrop beneath the deposit (Oliveira et al., 1995). In nearby stream beds and road/railway cuttings, the Série Negra rocks are rarely exposed. Several lenses of the Barreiros tectonised granitoid and thin cross-cutting rhyolite dykes can be seen in places.

In the São Martinho area, two stages of mineralisation are recognised (de Oliveira, 2001a, b; de Oliveira et al., 2001a): Early syntectonic Stage 1 (S1) and post-tectonic Late Stage 2 (S2) mineralization. S1 has the characteristics of a typical orogenic lode gold style of mineralization, showing disseminated mineralization with an ore paragenesis of pyrite I and II veinlets, stretched (deformed) pods of arsenopyrite I, chalcopyrite I and gold I, with marked chlorite alteration adjacent to the pyrite veinlets. Gold I is typically associated with pyrite II veinlets and grains are mostly <10 μm wide. S2 consists of massive mineralization and high-temperature sulphide minerals that cross-cut the regional foliation, with an ore paragenesis comprising pyrite III, arsenopyrite II (undeformed), pyrrhotite II, loellingite and gold II. S2 has higher gold grade (>1.5 g/t Au) than S1 (<1.0 g/t Au) and is important for regional gold exploration. Based on field relationships and available geochronology, S2 is interpreted to have occurred at *c.* 310 - 305 Ma, an age indicated by Bouchot et al. (2000) as the age of metalliferous peaks for Au, Sb and W mineralisation in western Europe. This age is also very close to that indicated for the emplacement of post-Hercynian granitoid magmas.

Both stages of gold mineralization are associated with very subtle alteration assemblages. Silicification, sericitization and chloritization are ubiquitous, but there are also vestiges of tourmalinization and albitization (de Oliveira, 2001a). Silicification is expressed in terms of two recognisable generations of quartz veins: quartz I (QI) and quartz II (QII). QI is early syntectonic quartz that is parallel or subparallel to the regional foliation and is associated with mineralizing event S1. Generally, QI veinlets are subtle and very narrow in core. QII is late quartz occurring as discrete, large and thicker veins cross-cutting the regional foliation of the Série Negra rocks and the veins are associated with S2. QII forms veins up to 35 cm in thickness, often with enclaves of quartz-biotite schist, visible gold and other sulphide minerals. The veins are responsible for much higher gold grades within the prospect area.

FLUID INCLUSIONS

Methodology

Fluid inclusions were measured using Fluid Inc. (Reynolds), Linkam PR600 and Linkam THMS600 (Lynksys 2.27), stages at the Instituto Geológico e Mineiro (IGM), the University of the Witwatersrand and the British Geological Survey (BGS), respectively. The stages were calibrated by measuring the precise melting point of CO_2 at -56.6 ºC in *Syn Flinc* synthetic fluid inclusions. Results obtained were found to be within <1 std. deviation of the mean for homogenization temperature (Th) from each type of instrument. The reproducibility of melting temperatures of ice (Tm_{ice}) and eutectic (Te) are better than 0.2 ^{o}C. Microthermometric data for fluid inclusions were collected with respect to petrographically

constrained fluid inclusion planes (FIP's) and measurements were carried out with respect to FIP's occupying the field of view of the 40x long-working-distance objective (c. 0.25 mm).

Fluid inclusions in FIP's from smaller broken chips of doubly polished wafers were mapped and selected for study. A cooling/heating rate of 0.2 ºC/min was used for cycling of the temperature at which the phase change occurred. In some cases it was impossible to obtain one precise temperature and instead, a range of temperatures was measured. Once the temperatures during the freezing runs were recorded, the chips were heated to observe homogenization temperatures of inclusions at 1º C/min. Cycling was also carried out to confirm the readings. In some cases, hypersaline inclusions homogenized at temperatures beyond the maximum limits set by the stages. At temperature >500 ºC some of the inclusions decrepitated. Calculations of salinity and pressures were made using published equations of state, namely, Bowers and Helgerson (1983) for H_2O-CO_2-NaCl inclusions, Zhang and Frantz (1987) for H_2O-NaCl inclusions and Sterner et al. (1988) for hypersaline inclusions.

Laser Raman spectroscopy using a Jobin-Yvon T6400 with an Olympus BX40 microscope attachment and a liquid-N_2 cooled CCD detector with an Ar ion laser (with 500mW power at the source) of 514.532 nm as excitation radiation, was used in single spectrograph mode to identify the gas species and daughter minerals within fluid inclusions. At the outset analyses proved difficult to obtain due to the small size of fluid inclusions. The lack of confocal optics, a system that reduces the length of the focal barrel (Murphy et al., 1998), coupled with the rough sample surface of particularly type E inclusions (see later) created problems with data acquisition.

Fluid inclusion types

On the basis of microscopic observation of individual and grouped fluid inclusion planes (FIP's) at room temperature, there is no evidence for any pristine primary fluid inclusions selected for study. All fluid inclusions are secondary or pseudosecondary. Five types of fluid inclusions at 25 ºC were recognized:

- Type A are leaked/stretched inclusions, rimming the edge of quartz grains in quartz I, and they were interpreted to be the remains of primary inclusions. The inclusions are generally very narrow, with a linear disposition, and can attain lengths of > 200 μm. Their microthermometric measurements were not obtained from these inclusions.

- Type B are extremely rare, dark monophase liquid CO_2 inclusions. They have a regular rounded-square shape, and are less than 6 μm in diameter and were only observed in QI although their occurrence in QII cannot be excluded.

- Type C, often found in QI, are mostly two-phase inclusions showing vapour>liquid (V>L; Fig. 3A). Within some FIP's some of the inclusions show only one phase (V or L), which can only be determined when the first phase change occurs under the heating-cooling run. The size of the inclusions is very small (3-4 μm) and is generally not suitable for study.

- Type D are also two-phase inclusions with L>V (Fig. 3B). Some of the inclusions average 5-6 μm, but most of them are < 5 μm. In very rare cases, inclusions of this type can be up to 15 μm. Their shape is generally regular and oval to round.

- Type E inclusions are considered to reflect an unusual fluid type giving the setting of the São Martinho gold prospect. They are mostly irregular in shape with daughter minerals (Fig. 3C) and typical of QII, although the fluids responsible for the inclusions are late and also heal cross-cutting fractures in QI.

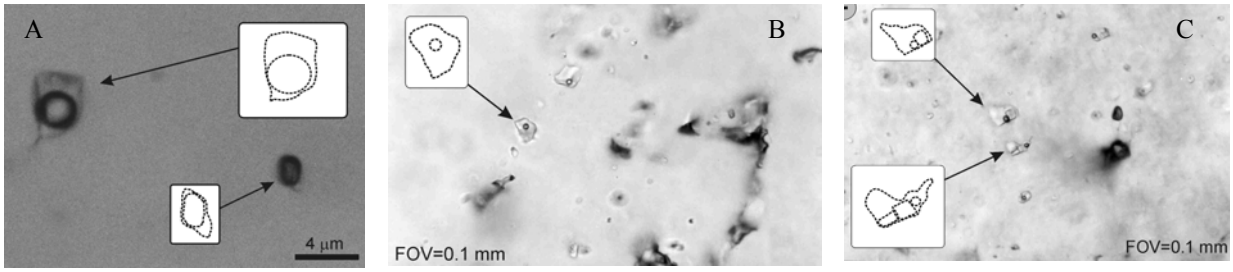

Figure 3: *Photomicrographic examples of fluid inclusion types found in the São Martinho gold prospect. A: Type C H_2O-NaCl-CO_2 -CH_4 fluid inclusions (V>L); B: Type D H_2O-NaCl fluid inclusions (L>V), and C: Type E hypersaline H_2O-NaCl fluid inclusions.*

In this study all the inclusions measured less than 21 µm in diameter. Inclusions measured are commonly 4-6 µm, rarely 6-10 µm and very rarely >10 µm. Some fluid inclusions, in particular FIP's, showed metastability phenomena where only two phases (L+V) were observed. However, they nucleated a daughter mineral with cyclical heating-cooling techniques. All the inclusions observed with respect to FIP's show constant V:L ratios and microthermometric data were obtained for types B, C, D and E.

The evidence for a temporal genetic relationship between ore and gangue minerals is the occurrence of fine-grained ore mineral inclusions within the gangue mineral itself or the inclusion of ore daughter minerals in the inclusions themselves (Wilkinson, 2001). Where such relationships are not observed at São Martinho, any inference of co-precipitation remains inconclusive, but probable. At São Martinho, the secondary and pseudosecondary fluid inclusions can be related to primary gold mineralization since the mineralization also occurs in fractures parallelling the FIP's (de Oliveira, 2001a; de Oliveira et al., 2001b).

The mode of occurrence, identification of the association between types of fluid inclusions and quartz generations, as well as the association of sulphide mineralization with FIP's of particular types of inclusions, indicate that inclusion types C and D are associated with S1 mineralization and inclusion type E is associated with S2 mineralization.

Microthermometric results

A summary of the microthermometric results for the São Martinho fluid inclusions is shown in Table 1.

Type B fluid inclusions, filled by 100% carbonic fluid, nucleated a vapour phase on cooling to between -40 and -30 ºC and showed bubble point homogenisation ($Th_{CO2(L)}$) between -0.9 and +7 ºC. Solid CO_2 in the inclusions melted (Tm_{CO2}) at approximately -60 ºC.

Type C fluid inclusions showed metastable phenomena and accurate temperatures of their equilibrium phase changes were difficult to obtain. However, freezing between -40 and +30 ºC commonly nucleated liquid CO_2 and, where observed accurately, dew point

homogenization of the carbonic component ($Th_{CO2(V)}$) occurred between -21 and +7 ºC (Table 1). Melting of solid CO_2 (Tm_{CO2}) occurred between -71 and -60 ºC with a mean temperature of -64.1 ºC (Table 1), indicating that the vapour phase contains significant amounts of other gases (e.g., CH_4: up to 30 mole%, see Raman results). CO_2 clathrate decomposition (Tm_{clath}) temperatures cannot be measured accurately because of the very small size of the inclusions, but occurred between 0 and 15 ºC. Detection of Th_{tot}, by disappearance of the aqueous phase ($Th_{(V)}$, dew point), carbonic phase ($Th_{(L)}$, bubble point) or critical behaviour, is between 245 and 521 ºC (Table 1). Two inclusions homogenized between 190 and 239 ºC. Critical behaviour was observed in inclusions that homogenized at approximately 415 ºC. Bubble point homogenization always occurred below this temperature at approximately 370 ºC, whilst dew point homogenization always occurred at >415 ºC to 521 ºC.

Type D fluid inclusions were solidly frozen at -58 ºC. Heating showed first melting temperature of ice (Te) between -52.6 and -38.7 ºC (Table 1). Further heating showed final melting of ice (Tm_{ice}) between -13 and +1.3 ºC (only 3 readings above 0 ºC, average -3.6 ºC, Table 1). The large range of Tm_{ice} may be due to observation errors as a result of the very small size of measured inclusions. However, it may also reflect a process of mixing of fluids with different salinities. $Th_{(L)}$ values are between 112 and 212 ºC (Table 1), but most lie between 112 and 162 ºC.

Table 1: Summary of the microthermometric results for fluid inclusions in vein quartz from mineralization stages 1-2 in the São Martinho prospect

Stage	Type	Microthermometric results (ºC)							
		Tm_{CO2}	$Th_{CO2(L)}$	$Th_{CO2(V)}$	Te	Tm_{ice}	Th_{tot}*	$Th_{(L)}$	Tm_{dau}
?	Type B (CO_2)	-60	-0.9 to +7	-	-	-	?	-	-
S1	Type C (H_2O-NaCl -CO_2-CH_4)	-71 to -60 (-64.1, n=20)	-	-21 to +7 (+2.3, n=18)	-	-	245 to 521 (371, n=28	-	-
S1	Type D (H_2O-NaCl)	-	-	-	-52.6 to –38.7 (-41.7, n=72)	-13 to +1.3 (-3.6, n=74)	-	112 to 212 (129, n=76)	-
S2	Type E (H_2O-NaCl) Hyper-saline	-	-	-	-	-	-	120 to 470 (290, n=161)	290 to >550 (400**, n=131)

* Th_{tot}, total homogenization temperatures, including homogenization to aqueous phase (bubble point), carbonic phase (dew point) and critical behaviour; ** 22 measurements over 550 ºC not included; Temperatures expressed as range and average (in brackets). n=number of inclusions.

Type E fluid inclusions produced no visible phase changes when frozen to -130 ºC. Daughter minerals melted (Tm_{dau}) between 290 and >550 ºC (average 400 ºC, n =131), although 22 measurements of >550 ºC are not included in this average, and $Th_{(L)}$ values fall in a range from 120 to 470 ºC (average 290 ºC, Table 1), which are lower than the Tm_{dau}.

Raman microspectrometric results

The observation of clathrate melting temperatures in type C inclusions indicates the presence of CO_2. However, the depressed melting temperature of CO_2 is beyond -56.6 ºC (at low pressure, 0.5 Mpa, the triple point of pure CO_2; Diamond, 2001), which indicates the presence of other gaseous compounds (Nabelek and Ternes, 1997; Kerkhof and Thiéry, 2001). Using graphical estimates (Shepherd et al., 1985), the type C inclusions contain approximately 20 mole% CH_4. Raman analysis of 20 inclusions, averaging 2-4 μm across, showed the quartz to be strongly fluorescent, which causes a background signal that masks all but the strongest peaks. Since CH_4 is a strong Raman scatterer it appears above the background fluorescence. CO_2 shows a much weaker signal and is easily masked by the background. The use of the 488 nm excitation line yielded molar ratios of CO_2:CH_4 of 70:30 (n =3).

The Tm_{ice} values of type D inclusions (-13 to +1.3 ºC) are indicative of the presence of H_2O with NaCl and gas hydrates, depressing the melting point of ice above 0 ºC. Raman analysis was tried on the inclusions both to confirm suspected observations and to bring out new data. The small size and mobile bubble of type D inclusions made Raman analysis very difficult. However, the Raman showed that the fluids comprise H_2O and hydrated salts (divalent cations; $CaCl_2$?). No further clue was obtained with respect to the identity of the salts using Raman spectroscopy. NaCl is present, although it does not have a Raman spectrum. The Te values (-52.6 to -38.7 ºC) indicate that the hydrated salts are mixtures of NaCl-$MgCl_2$. However, H_2O vapour was the only compound detected.

The only real clues as to their chemistry of type E inclusions, due to their inability to show phase changes during microthermometry, were to be obtained using Raman spectroscopic techniques. The gaseous bubble was identified as H_2O vapour. However, the spectra showed the possible presence of Mg, Ca, CO_3 and SO_4, huntite [$Mg_3\,Ca(CO_3)_4$], $CaSO_4$ and $Ca(OH)_2$ (Nieuwoudt, 2000). Traces of N_2 were also detected that were too small to be quantified. The fluid showed a H_2O + hydrated salts (NaCl-KCl) composition. The daughter crystals showed a confusing array of Raman spectra, and the possible presence of Mg, K, Fe and $CaCO_3$.

DISCUSSION

Salinity-Th correlation

S1 mineralisation: Salinities for type C inclusions have limited precision because of the very small size of fluid inclusions and the limit to which phase changes could be observed (e.g., CO_2 clathrate). Using the Bowers and Helgerson (1983) method, a mean salinity of approximately 10 wt.% NaCl equivalent was estimated (Fig. 4A). The method of calculation relies on precise Tm_{clath} measurements and the Tm_{clath} obtained in this study ranges between 0 and 15 ºC. The upper interval of this bracket is probably overestimated even with slow heating rates of < 1 ºC/min. Hence, a median value of 5 ºC was chosen for calculation purposes. Also, the presence of volatiles (e.g., CH_4) will cause Tm_{clath} to be higher and conversely salinity will be lower than the recorded value. The salinity estimated by this method is considered to be a maximum for the fluid inclusions analysed. Thus, the choice of a median value of 5 ºC seems justified. Salinity values for type D inclusions were estimated to fall in a range from 0.5 to 17.2 wt.% NaCl equivalent (Figs. 4A, B), using the method of Zhang and Frantz (1987).

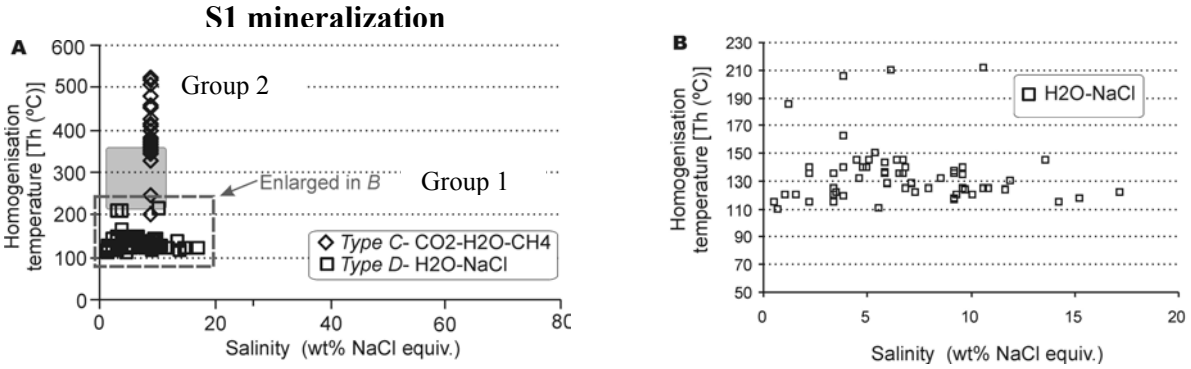

Figure 4: *A: Salinity (wt.% NaCl equiv.) vs. homogenization temperature graphs for types C and D fluid inclusions. The grey box represents the area of occurrence of fluid inclusions from mesothermal lode gold deposits (after Wilkinson, 2001). B shows the detail of the spread of data for the type D fluid inclusions that may be indicative of mixing.*

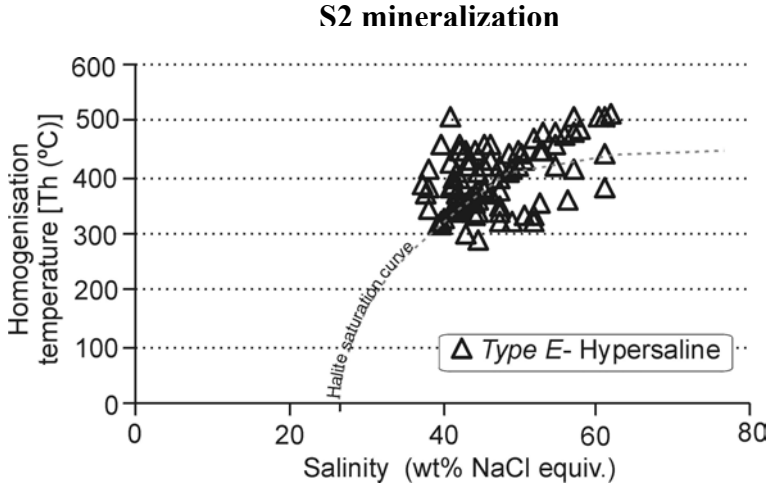

Figure 5: *Salinity (wt.% NaCl equiv.) vs. homogenization temperature graphs for type E fluid inclusions showing that most of these fluid inclusions homogenize by halite dissolution. A few inclusions (22%) were observed to homogenize by bubble homogenization.*

Two groups of salinities are shown in Figure 4A. Group 1 is composed of type D inclusions (salinities: 0.5 to 17.2 wt% NaCl equivalent, T_h: 112-212 ºC). This group possibly reflects high-salinity fluids mixed with low-salinity fluids (<0.5 wt.% NaCl equivalent) at low temperature (<150 ^oC). Group 2, composed of type C fluid inclusions, show estimated average salinities of ±10 wt% NaCl equivalent and T_h of 245-510 ºC. This group of fluid inclusions is possibly trapped from high-temperature (>500 ^oC), moderate salinity (>15 wt.% NaCl equivalent) fluids mixed with low-temperature (<200 ^oC) and low-salinity (<0.5 wt.% NaCl equivalent) fluids in an open system.

S2 mineralization: Type E inclusions: Salinity values for the multiphase hypersaline inclusions in the São Martinho prospect were calculated using the equation of Sterner et al. (1988) based on halite dissolution temperatures (Tm_{dau}). Accordingly, salinities for the inclusions vary between 32 and 62 wt.% NaCl equivalent (Fig. 5). However, the true salinity range will be larger since the higher Tm_{dau}> 550 ºC were not attained due to equipment limitations and hence, Figure 5 does not reflect the total number of data.

In terms of the fluids responsible for the S2 stage of mineralization in the São Martinho area, type E fluid inclusions occur either side of the halite saturation curve as well as on the curve itself (Fig. 5). Those inclusions that lie on the halite saturation curve seemingly represent the true trapping of fluid inclusions, while those that lie outside the curve may have been modified after trapping.

In general, it appears that two types of fluids existed: (1) high-salinity (>60 wt.% NaCl equivalent) fluids as indicated by type E inclusions from QII; and (2) moderate-salinity (<17 wt.% NaCl equivalent) fluids as demonstrated by types C-D fluid inclusions from QI. At low temperature (<150 ^{o}C), the types C-D inclusions were mixed with addition of very low-salinity (<0.5 wt.% NaCl equivalent) fluids.

Hypersaline fluid inclusions

Hypersaline fluid inclusions with high homogenization temperatures are common in porphyry copper environments (i.e., magmatic environments) and have been recorded in 90% of the deposits studied (e.g., Arribas et al., 1995; amongst others). Bodnar (1995) reported that fluid inclusions in a porphyry copper deposit are high salinity, halite-bearing inclusions that homogenize at relatively high temperatures (>500-600 ºC). Some authors viewed the inclusions as a result of boiling of high temperature fluid or immiscible vapour derived directly from shallow-emplaced magmas (Hedenquist and Lowenstern, 1994; amongst others).

Daughter minerals have rarely been reported in orogenic lode gold (mesothermal) environments, and hence should be unusual in settings such as the São Martinho prospect, although dawsonite [$NaAlCO_3(OH_2)$] has been documented by Coveney and Kelley (1971). Nevertheless, fluid inclusions with distinct halite (+KCl) crystals form a predominant part of the inclusion population, both in terms of size and abundance, and are by far the most important inclusions associated with significant gold mineralisation in the São Martinho area.

At São Martinho, hypersaline, daughter mineral-bearing fluid inclusions are trapped from fluids responsible for late remobilized mineralization (S2), which is overprinted on early syn-tectonic lode gold (S1). The fluid inclusions are typically hosted in late (post-tectonic or post-Hercynian) structures. Hence, their origin is likely to be magmatic. The late magmas recognized in the region are the late-post Hercynian granites (e.g., Nisa and Stª Eulália as well as rhyolites east of the São Martinho area). The hypersaline fluids therefore indicate overprinting of early lode gold mineralization by late magmatic fluids, a feature that has been recognized in orogenic lode gold deposits before (Bierlein and Crowe, 2000). Since the hypersaline fluid inclusions occur in late QII veins, their presence can be used as an important indicator of the presence of higher gold grades in the São Martinho and adjacent areas within the TCSZ and, hence, be a useful exploration tool.

Estimate of P-T conditions

Homogenization temperatures are usually a minimum estimate of trapping temperatures. Pressure estimates rely heavily on the composition of the fluid and its PVTX properties. Composition is seldom easy to establish, except in terms of its major components (H_2O, NaCl, CO_2).

In this study, the trapping pressures were estimated using calculated isochores and independent geothermometers (336 and 400 ºC) estimated from hydrothermal chlorite associated with pyrite II veinlets (de Oliveira, 2001a) in S1. A mean temperature of 368 ºC was used, which, for type C fluid inclusions, is very close to the median temperature (371 ºC). Results show that the estimated trapping pressures are between 4.3 and 6.2 kbar using the mean, but between 3.8 and 7 kbar using ± 1x std. deviation, which are comparable with published data on the metamorphic conditions of the Série Negra rocks that formed in peak metamorphic conditions at 680 ºC and 6-8 kbar and 350-400 ºC and 7-8 kbar on garnets extracted from the Unidad de la Cuartel amphibolites (Abalos Vilaro, 1992). The *P-T* data (400-500 ^{o}C and 4 -7 kbar) from the São Martinho prospect are significantly higher than those from most mesothermal lode gold deposits (commonly 250-350 ºC and 1 kbar: Hagemann and Cassidy, 2000; Bierlein and Crowe, 2000; 300-450 ^{o}C and 3 kbar; Ryan and Smith, 1998), indicating that the S1 style of mineralization was formed at relatively high P-T.

In terms of S2 mineralization, the calculation of isochores and their slopes in a phase change diagram cannot be determined since equations of state for multi-cations systems are unknown (Campbell, 1995). High salinity (> 60 wt.% NaCl equiv.) L+S fluid inclusions that homogenize by daughter mineral dissolution, in a P-T diagram (e.g., Sterner et al., 1988) would only nucleate a vapour bubble at relatively low pressures (< 1 kb). Given the characteristics of the high salinity fluid inclusion population, and the structural evolution of the TCSZ, an area that underwent continuous uplift and erosion, it is estimated that the trapping pressures of type E fluid inclusions are probably lower than those associated with S1 mineralisation.

Sources of fluids

Generally, the hydrothermal fluids responsible for the formation of orogenic lode gold deposits are characterised by low pH and uniformly low salinities (<5-6 wt % NaCl equivalent, Bierlein and Crowe, 2000; Hagemann and Cassidy, 2000), although salinities in excess of 10 wt.% NaCl equivalent have been also observed in some deposits (e.g., So and Yun, 1997). Consequently, daughter minerals in fluid inclusions (hypersaline fluid inclusions) are rare (Bierlein and Crowe, 2000) as stated previously. The fluids usually contain 5 and 50 mole% CO_2 and < 5 mole% CH_4 (Bierlein and Crowe, 2000). Traces of N_2 have been identified in fluid inclusions from some Au-Sb-As deposits in the west Lachlan orogen (Gao and Kwak, 1995) and in the Alaskan cordillera (Miller et al., 1995).

The data from the São Martinho prospect indicates that the mineralizing fluids associated with early (S1) orogenic lode gold mineralization are generally dilute fluids containing CO_2 (up to 70 mole%) and CH_4 (up to 30 mole%). Salinities vary from 0.5 to 17.2 wt.% NaCl equivalent. Although some variation does occur, the early mineralizing fluids can be considered to fit within the parameters highlighted by Bierlein and Crowe (2000) for orogenic lode gold deposits. Given the geochronological constraints of the mineralization in light of the host rocks (Série Negra) and the spatial relationships that it exhibits with both syn- and post-tectonic granitoid bodies, the fluid source is probably derived from mixing of metamorphic fluids with fluids generated from syntectonic granitoid magmas.

Metamorphic dehydration reactions in pelites of the Série Negra (Azuaga and Atalaya Formations) have been documented on the Spanish side of the Tomar Cordoba Shear Zone by Abalos Vilaro (1992) and include:

* chlorite + K-feldspar = biotite + chlorite + quartz + H_2O

* 3 phengite + chlorite = 3 biotite + 7 quartz + 4 H_2O, and

* chlorite + biotite 1 + quartz = garnet + biotite 2 + H_2O

Reactions of this type can supply (ore-forming) metamorphic fluids in geological environments such as the São Martinho prospect.

As discussed above, the hypersaline fluids responsible for high-grade gold mineralization (S2) are thought to be derived from late, post-tectonic/Hercynian magmas. The suggestion is also clearly supported by the geology. The São Martinho area is close to the contact with the Nisa Batholith to the west and also the presence of granitoid suboutcropping beneath the elluvium deposit. It is likely that the S2 mineralizing fluids were derived from magmas that eventually formed the Nisa Batholith.

CONCLUSIONS

Two distinct stages of mineralization in the São Martinho prospect are:

(1) a syntectonic, orogenic lode gold type (S1) at 400-500 ^oC and 4 -7 kbar; and

(2) a post-tectonic, magmatic, higher temperature (>500ºC, P<4-7 kbar) type (S2).

QI veinlets contain secondary/pseudosecondary fluid inclusions of types C (H_2O-NaCl-CO_2-CH_4) and D (H_2O-NaCl). The salinities of both types of fluid inclusions varies from 0.5 to 17.2 wt% NaCl equivalent. The fluids probably originated as a result of metamorphic devolatilization reactions within the Série Negra host rocks. However, the microthermometric data also indicate that fluid mixing is likely to act in an open system between moderate salinity (<17 wt.% NaCl equivalent), high temperature (>500 ^oC) fluids with low temperature (<150 ^oC), low salinity (<0.5 wt.% NaCl equivalent) fluids.

QII veins mainly contain secondary/pseudosecondary daughter mineral-bearing, hypersaline fluid inclusions (type E). Raman analysis of type E inclusions proved inconclusive although the gaseous bubbles in the inclusions are largely composed of H_2O with traces of N_2, the liquid portion yields Raman spectra of H_2O + hydrated salts (NaCl-KCl) and the daughter minerals show a confusing array of overlap spectra for Mg, K, Fe and $CaCO_3$. The source of the high temperature (>500 ^oC), hypersaline fluids (>60 wt.% NaCl equivalent) is probably derived from the emplacement of Upper Westphalian post-tectonic granitoid magmas, where the N-S tension fractures/gashes are prominent in the region.

At São Martinho the original lode gold system (S1) resulted in a low-potential, low-grade gold occurrence, which was up-graded to an area of higher grades of gold mineralization by remobilization of S1 lode gold by later magmatic fluids. Since QII veins are associated with more massive-style sulphide mineralization and also visible gold, the identification of hypersaline fluid inclusions and hence, QII, can be used as an exploration tool in the area.

ACKNOWLEDGEMENTS

This research represents part of a Ph.D study undertaken at the University of the Witwatersrand (WITS), Republic of South Africa and in the Instituto Geológico e Mineiro (IGM), Portugal. The senior author benefited from a *Praxis XXI* Ph.D bursary (BD/15877/98) awarded by the *Fundação para a Ciência e a Tecnologia (Ministério da Ciência e do Ensino Superior, Portugal)*. Mr. J. L. Pinto (IGM) helped with sample collection and field work and Mr. A. Mathebula (WITS) prepared the doubly polished thin sections used in the study. Ms M. Nieuwoudt of the National Raman Spectroscopy and Cathodoluminescence Laboratory is thanked for help with Raman analysis of fluid inclusions at WITS.

REFERENCES

Abalos, B. and Eguiluz, L., 1992. The late Proterozoic suture zone of SW Iberia: a link for the reconstruction of the Cadomian-Avalonian-Panafrican transpressive orogen of the Circum-Atlantic region. Comptes Rendus de l'Académie des Sciences, t. 314, Série II, 691-698.

Abalos Vilaro, B., 1992. Cinematica y mecanismos de la deformacion en regimen de transpresion. Evolucion estrutural y metamorfica de la zona de cizalla ductil de Badajoz Cordoba. Serie NOVA TERRA, Nº6. Edicios do Castro, 430 p.

Arribas, Jr., A., Cunninham, C.G., Rytuba, J.J., Rye, R.O., Kelly, W.C., Podwysocki, M.H., McKee, E.H. and Tosdal, R.M., 1995. Geology, geochronology, fluid inclusions and isotope geochemistry of the Rodalquilar gold alunite deposit, Spain. Economic Geology, 90, 795-822.

Berthé, D, Choukroune, P and Jegouzo, P., 1979. Orthogneiss, mylonite and non coaxial deformation granites: the example of the south Armorican shear zone. Journal of Structural Geology, 1, p31-42.

Bierlein, F.P. and Crowe, D.E., 2000. Phanerozoic orogenic lode gold deposits. *In:* Hagemann, S.G. and Brown, P.E. (eds.), *Gold in 2000*. Reviews in Economic Geology, 13, 103-139.

Bodnar, R.J., 1995. Fluid-inclusion evidence for a magmatic source of metals in porphyry copper deposits. *In:* Thompson, J.F.H. (ed.), *Magmas, Fluids and Ore Deposits*. Mineralogical Association of Canada Short Course Series, 23, 139-152.

Bouchot, V., Milesi, J.P. and Ledru, P., 2000. Crustal-scale hydrothermal palaeofield and related Variscan Au, Sb, W orogenic deposits at 310-305 Ma (French Massif Central, Variscan Belt). Society for Geology Applied to Mineral Deposits (SGA) News, Dec. 2000, Nº 10, p1, 6-12.

Bowers, T.C. and Helgerson, H.C., 1983. Calculation of the thermodynamic and geochemical consequences of nonideal mixing in the system H_2O-CO_2-NaCl on phase relations in geologic system: Equation of state for H_2O-CO_2-NaCl fluids at high pressures and temperatures. Geochimica et Cosmochimica Acta, 47, 1247-1275.

Burg, J.P., Iglesias, M., Laurent, P.H., Matte, P. and Ribeiro, A., 1981. Variscan intracontinental deformation: the Coimbra-Córdoba Shear Zone (SW Iberian Peninsula). Tectonophysics, 78, p161-177.

Camm, G.S., 1996. Report on the surficial hardrock exploration for gold mineralization in the São Martinho area, Portalegre, Portugal. Auspex Minerals Ltd. (internal report).

Campbell, A.R., 1995. The evolution of a magmatic fluid: a case history from the Capitan mountains, New Mexico. *In:* Thompson, J.F.H. (ed.), *Magmas, Fluids and Ore Deposits*. Mineralogical Association of Canada Short Course Series, 23, 291-308.

Couture, J-F., Pilote, P. and Machado, N., 1994. Timing of gold mineralisation on the Val d'Or district, southern Abitibi Belt: evidence for two distinct mineralizing events. Economic Geology, 89, 1542-1551.

Coveney, R.M.Jr. and Kelley, W.C., 1976. Dawsonite as a daughter mineral in hydrothermal fluid inclusions. Contributions to Mineralogy and Petrology, 32, 334-342.

de Oliveira, D.P.S., 2001a. The nature and origin of gold mineralisation in the Tomar Cordoba Shear Zone, Ossa Morena Zone, East central Portugal. PhD thesis (unpubl.), University of the Witwatersrand, Johannesburg, South Africa, 352pp.

de Oliveira, D.P.S., 2001b. Primary lode gold mineralisation vs. magmatically remobilised gold mineralisation at São Martinho (Tomar Cordoba Shear Zone): its timing deduced from structural relationships. *In: Livro das apresentações científicas e livro-guia de excursão,* 7ª Conferência Anual do Grupo de Geologia Estrutural e Tectónica (GGET2001), p51-54.

de Oliveira, D.P.S., Robb, L.J. and Inverno, C.M.C., 2001a. The São Martinho gold occurrence, NE Ossa Morena Zone, Portugal: geological setting and ore genesis. *In:* Piestrzynski et al., (eds.), *Mineral Deposits at the Beginning of the 21st Century,* Proceedings of the Joint Sixth Biennial SGA-SEG Meeting/Kraków, Poland/26-29 August 2001, 791-793.

de Oliveira, D.P.S., Shepherd, T., Naden, J. and Yao, Y., 2001b. Evidence for a late magmatic gold remobilising event in a mesothermal temperature setting at São Martinho, NE Ossa Morena Zone, Portugal. *In:* Noronha, F., Dória, A. and Guedes, A. (eds.). *ECROFI XVI European Current Research On Fluid Inclusions* - Abstracts, Universidade do Porto, Fac. de Ciências, Depto. de Geologia. Memórias nº7, 349-351.

de Oliveira, D.P.S., Poujol, M. and Robb, L.J., 2002. U-Pb geochronology for the Barreiros tectonised granitoids and Arronches migmatitic gneisses: Tomar Cordoba Shear Zone, east central Portugal. Rev. Soc. Geol. España 15 (1-2): 105-112.

Diamond, L.W., 2001. Review of the systematics of CO_2-H_2O fluid inclusions. Lithos, 55, 69-99.

Gao, Z.L. and Kwak., T.A.P., 1995. Turbidite-hosted gold deposits in the Bendigo-Ballarat and Melbourne zones, Australia. I. Geology, mineralisation, stable isotopes, and implications for exploration. International Geology Review, 37, 910-944.

Gonçalves, F., Perdigão, J. C., Coelho, A. V. P. and Munhá, J. M., 1978. Notícia explicativa da folha 33-A (Assumar). Serviços Geológicos de Portugal, 37pp.

Hagemann, S.G. and Cassidy, K.F., 2000. Archean orogenic lode gold deposits. *In:* Hagemann, S.G. and Brown, P.E. (eds.), *Gold in 2000*. Reviews in Economic Geology, 13, 9-68.

Hedenquist, J.W. and Lowenstern, J.B., 1994. The role of magmas in the formation of hydrothermal ore deposits. Nature, 370, 519-527.

Julivert, M., Fontboé, J.M., Ribeiro, A. and Conde, L.N., 1972. Mapa Tectónico de la Peninsula Ibérica y Baleares. Intituto Geologico y Minero de España, Madrid, 101pp.

Kerkhof, A.v.d. and Thiéry, R., 2001. Carbonic inclusions. Lithos, 55, 49-68.

Miller, L.D., Goldfarb, R.J., Snee, L.W., Gent, C.A. and Kirkham, R.A., 1995. Structural geology, age, and mechanisms of gold vein formation at the Kensington and Julian deposits, Berners Bay District, southeast Alaska. Economic Geology, 90, 343-368.

Moreira, A., 1994. Reconhecimento geológico, estrutural, petrográfico e geoquímico dos granitos de Alpalhão, Gáfete e Quarteleiros (Alto Alentejo). Estudos, Notas e Trabalhos, IGM, t.36, 103-117.

Murphy, P.J., Stevens, G. and Lagrange, M.S., 1998. Geological applications of Raman spectroscopy and the use of Raman spectroscopy in the study of gold speciation in fluids. Information Circular, Economic Geology Research Unit, University of the Witwatersrand, Johannesburg, 321, 41pp.

Nabelek, P.I. and Ternes, K., 1997. Fluid inclusions in the Harney Peak Granite, Black Hills, South Dakota, USA: implications for solubility and evolution of magmatic volatiles and crystallisation of leucogranite magmas. Geochimica et Cosmochimica Acta, 61, 1447-1465.

Nieuwoudt, M., 2000. Raman analysis of fluid inclusions TPMN, HSMN, HSD and DP27. Raman Laboratory report (unpubl.), Dept. of Physics, University of the Witwatersrand, Johannesburg, 48pp.

Oliveira, J.T., Pereira, E., Ramalho, M., Antunes, M. T. and Monteiro, J .H., 1992. Geological Map of Portugal, 1: 500 000. Serviços Geológicos de Portugal.

Oliveira, D.P.S., Martins, L.M.P. and Viegas, L.F.S., 1995. Gold mineralization occurrences in the Crato-Campo Maior sector of the Blastomylonitic Zone (northern Alentejo, Portugal). Estudos, Notas e Trabalhos, IGM, t. 37, 113-122.

Ordoñes-Casado, B., 1998. Geochronological studies of the Pre-Mesozoic basement of the Iberian Massif: the Ossa Morena Zone and the allochthonous complexes within the Central Iberian Zone. Ph.D thesis (unpubl.), Swiss Federal Institute of Technology Zürich (ETH), Nº 12.940, 233pp.

Pereira, M.F.C. de C., 1995. Estudo tectónico da megaestrutura de Crato-Arronches-Campo Maior: A Faixa Blastomilinítica e limite setentrional da Zona de Ossa Morena com o autóctone Centro Ibérico (Nordeste Alentejano). M.Sc thesis (unpubl.), Faculty of Science, University of Lisbon, 108pp.

Pereira, F. and Silva, J.B., 1997. A estrutura nos domínios setentrionais da Zona de Ossa Morena: A Faixa Blastominonítica e a Zona de Transição com o Autóctone Centro-Ibérico (Nordeste Alentejano-Portugal). *In:* Araújo, A.A. and Pereira, M.F. (eds.), *Estudo Sobre a Geologia de Ossa Morena (Maciço Ibérico),* Homenagem ao Prof. Francisco Gonçalves, Universidade de Évora, p. 183-204.

Pereira, M. F. and Silva, J.B., 2001. A new model for the Hercynian Orogen of Gondwanan France and Iberia: discussion. Journal of Structural Geology, 23, 835-838.

Pereira, M.F.C. de C., 1999. Caracterização da estrutura dos domínios setentrionais da Zona de Ossa Morena e seu limite com a Zona Centro ibérica, no nordeste alentejano. Ph.D thesis (unpubl.), University of Évora, 114 pp.

Quesada, C. and Munhá, J., 1990. *In:* Dallmeyer, R.D. and Martinez Garcia, E. (eds.), *Pre-Mesozoic Geology of Iberia*, Springer-Verlag Berlin, p. 314-319.

Ribeiro, A., Antunes, M.T., Ferreira, M.P., Rocha, R.B., Soares, A.F., Zbyszewski, G., Almeida, F.M. de, Carvalho, D. de and Monteiro, J.H., 1979. Introduction à la géologie générale du Portugal, Serviços Geológicos de Portugal, 114pp.

Ridley, J.R. and Diamond, L.W., 2000. Fluid chemistry of orogenic lode gold deposits and implications for genetic models. Society of Economic Geology Reviews, 13, 141-162.

Ryan, R.J. and Smith, P.K., 1998. Gold mineralisation in Nova Scotia. Ore Geology Reviews, 13, 153-183.

Shepherd, T.J., Rankin, A.H. and Alderton, D.H.M., 1985. A practical guide to fluid inclusions. Blackie, London, 239pp.

So, C.-S. and Yun, S.-T., 1997. Jurassic mesothermal gold mineralisation of the Samhwanghak Mine, Youngdong area, Republic of Korea: constraints on hydrothermal fluid geochemistry. Economic Geology, 92, 60-80.

Sterner, S.M., Hall, D.L. and Bodnar, R.J., 1988. Synthetic fluid inclusions. V. Solubility relations in the system NaCl-KCl-H_2O under vapour-saturated conditions. Geochimica et Cosmochimica Acta, 52, 989-1005.

Wilkinson, J.J., 2001. Fluid inclusions in hydrothermal ore deposits. Lithos, 55, 229-272.

Yao, Y., Murphy, P.J. and Robb, L.J., 2001. Fluid characteristics of granitoid-hosted gold deposits in the Birimian Terrane of Ghana: a fluid inclusion microthermometric and Raman spectroscopic study. Economic Geology, 96, 1611-1643.

Zhang, Y.-G. and Frantz, J.D., 1987. Determination of the homogenisation temperatures and densities of supercritical fluids in the system NaCl-KCl-$CaCl_2$-H_2O using synthetic fluid inclusions. Chemical Geology, 64, 335-350.

_____oOo_____